Italian Journal of Food Science, 2024; 36 (3): 291–300

Kaempferol-3-O-rutinoside protects myocardial cell injury by inhibiting the TXNIP/NLRP3 pathway

Ling-li Shi[1], Xiao-ni Zhao[2], Juan Bai[1], Sheng-nan Li[1], Fang Hua[1]*, Peng Zhou[2]*

[1]School of Pharmacy, Anhui Xinhua University, Anhui, P.R. China; [2]Department of Integrated Traditional Chinese and Western Medicine, Anhui University of Chinese Medicine, Anhui, P.R.China

***Corresponding Authors:** Fang Hua, School of Pharmacy, Anhui Xinhua University, Anhui, P.R. China. Email: happyhf6941@sina.com; Peng Zhou, Department of Integrated Traditional Chinese and Western Medicine, Anhui University of Chinese Medicine, Anhui, P.R.China. Email: zhoupeng@ahtcm.edu.cn

Received: 20 June 2024; Accepted: 23 July 2024; Published: 13 August 2024

ORIGINAL ARTICLE

Abstract

Kaempferol-3-O-rutinoside (KR), a compound commonly found in green tea, has demonstrated significant myocardial protective effects. The aim of this study was to reveal the cardioprotective mechanism of KR. In this study, molecular docking was employed to predict the binding affinity of KR to thioredoxin-interacting protein (TXNIP). An injury model of H9c2 cells was established using lipopolysaccharide (LPS) and adenosine triphosphate (ATP). Lactate dehydrogenase (LDH) levels were measured using specific kits, while total superoxide dismutase (T-SOD), malondialdehyde (MDA), glutathione (GSH), and catalase (CAT) activities were assessed with colorimetric assays. The reactive oxygen species (ROS) level was determined using the DCFH-DA fluorescent probe assay. In addition, the expression levels of TXNIP, NLR-family pyrin domain-containing protein 3 (NLRP3), cysteinyl aspartate specific proteinase-1 (Caspase-1), and thioredoxin (TRX) were quantified by reverse transcription polymerase chain reaction (RT-PCR) and Western blot (WB) assays. Levels of interleukin-1β (IL-1β) and IL-18 were determined by ELISA. The results indicated that KR has a specific binding affinity for TXNIP. KR was found to reduce LDH and MDA activities, increase CAT, GSH, T-SOD, and inhibit ROS production. Mechanistically, KR decreased the gene and protein expressions of TXNIP, Caspase-1, and NLRP3, while increasing the gene and protein expression of TRX. Also, KR decreased the levels of IL-1β and IL-18. In conclusion, the protective mechanism of KR against cardiomyocyte injury involves the inhibition of the TXNIP/NLRP3 pathway, providing experimental evidence for its potential clinical application.

Keywords: Kaempferol-3-O-rutinoside; molecular docking; myocardial cell injury; TXNIP/NLRP3 pathway

Introduction

The term "myocardial infarction" refers to the damage to vulnerable atherosclerotic plaques or the erosion of coronary artery endothelial cells (Palasubramaniam *et al.*, 2019). When cardiomyocytes die, they release specific proteins that trigger inflammatory responses in the myocardium (Frangogiannis, 2014). During acute myocardial infarction, cardiomyocytes can produce large amounts of reactive oxygen species (ROS), which significantly contribute to oxidative stress (Zheng *et al.*, 2022). In recent years, it has been discovered that ROS not only cause oxidative stress but also act as an important inflammatory signal, playing a key role in activating the NLR-family pyrin domain-containing protein 3 (NLRP3) inflammasome (Wang *et al.*, 2020). In the absence of stimulation, thioredoxin-interacting protein (TXNIP) binds to the thioredoxin (TRX), inhibiting its activity (Yoshihara *et al.*, 2024). When cells are stimulated by external signals and mitochondrial ROS release is increased, this complex dissociates. TXNIP then binds to NLRP3 inflammasome, activating the NLRP3 inflammasome, which

leads to an increase in cytokine secretion. This activation triggers downstream inflammatory responses that results in pyroptosis and ultimately cause cardiomyocyte injury (Cheng *et al.*, 2020; Zhao *et al.*, 2023).

Kaempferol-3-O-rutinoside (KR), commonly present in green tea, exhibits significant pharmacological activities, including anti-liver injury, anti-cerebral ischemia/reperfusion injury, anti-multi-infarct dementia, anti-hyperglycemia, and anti-coronavirus 2019 (COVID-19) (Dubey and Dubey, 2021; Hua *et al.*, 2018; Petpiroon *et al.*, 2015; Wang *et al.,* 2015). Previous studies have found that KR is the most abundant flavonoid glycoside in Chinese traditional tea, Lu'an GuaPian tea (Hua *et al.*, 2018). The flavonoid glycoside derivatives in Lu'an GuaPian tea showed good inhibition of lipid accumulation in 3T3-L1 adipocytes (Bai *et al.*, 2017). Additionally, these derivatives exhibited strong inhibitory effects on α-glucosidase and α-amylase, among which KR showed a particularly strong inhibition of α-amylase through hydrogen-bonding interactions (Hua *et al.*, 2018). KR has demonstrated obvious anti-inflammatory effects, particularly in protecting H9c2 cardiomyocytes from lipopolysaccharide (LPS)-induced inflammatory injury. It significantly increases cell survival and downregulates the protein expression levels of toll-like receptor 4 (TLR4), myeloid differentiation primary response 88 (MyD88), and nuclear factor kappa-B (NF-κB) (Hua *et al.*, 2021). Recent studies have also shown that KR had good therapeutic effects on rats in a model of ventricular remodeling (VR) following acute myocardial infarction (AMI). It significantly improves cardiac function and hemodynamic indexes, reduces pathological changes and myocardial fibrosis, and inhibits the overexpression of NLRR3, cysteinyl aspartate specific proteinase-1 (Caspase-1), and gasdermin D (GSDMD) (Hua *et al.*, 2022). The NLRP3 signaling pathway is closely related to its upstream ROS/TXNIP pathway (Zhu *et al.*, 2024). KR regulates inflammation and inhibits cellular pyroptosis by inhibiting the ROS/TXNIP signaling pathway. However, the effect of KR on VR after AMI is unclear. The present study aims to further investigate this mechanism.

Molecular docking is a method of drug design that involves characterizing the receptor and the interaction mode between the receptor and the drug. It can also be used to predict the possible targets of drugs and to clarify their mechanism of action (Guedes *et al.*, 2014). In recent years, molecular docking has become a valuable technique for studying the mechanisms of traditional Chinese medicine combinations (Zhou *et al.*, 2023). Combining molecular docking with experimental validation can better elucidate the mechanisms by which traditional Chinese medicines act against diseases.

In this study, we used molecular docking to predict the binding affinity of KR and TXNIP. We then conducted modern morphology and molecular biology experiments to observe the effects of KR on the expression of key proteins and genes in the model of cardiomyocyte pyroptosis mediated by the ROS/TXNIP/NLRP3 pathway. Our aim was to define the mechanism through which KR prevents and treats cardiomyocyte pyroptosis, providing experimental evidence for the clinical application and popularization of natural products.

Materials and Methods

Cell

The H9c2 cell line was purchased from Procell Life Technology Co. Ltd. (Wuhan, China).

Chemicals and regents

Kaempferol-3-O-rutinoside was purchased from Shanghai Yuanye Bio-Technology Company (Shanghai, China). Lipopolysaccharide (LPS) (L8880) was purchased from Technology Co. Ltd (Beijing, China). Adenosine triphosphate (ATP) (A832633) was purchased from Macklin Biochemical Technology Co. Ltd (Shanghai, China). Lactate dehydrogenase (LDH) (A020-2-2), malondialdehyde (MDA) (A003-1-2), total superoxide dismutase (T-SOD) (A001-1-2), catalase (CAT) (A007-1-1), and glutathione (GSH) (A006-2-1) were purchased from Nanjing Jiancheng Bioengineering Insitute (Nanjing, China). Interleukin (IL)-1β (MM-0047R2) and IL-18 (MM-0194R2) were bought from Meimian (Jiangsu, China). ROS kit (CA1410) was purchased from Solarbio Inc. Anti-TXNIP (DF7506) and anti-Cleaved-caspase-1 (AF4005) were purchased from Affinity Biosciences. Anti-TRX (ab273877) and anti-NLRP3 (ab263899) were obtained from Abcam. Penicillin-streptomycin solution (BL505A) was purchased from Biosharp (China).

Culture of H9c2 cells

H9c2 cells were cultured in DMEM medium supplemented with 10% fetal bovine serum (FBS) and 1% penicillin-streptomycin solution. The cells were maintained at 37°C, 5% CO_2, and 85%–95% relative humidity.

H9c2 cell treatment

In 6-well plates, H9c2 cells were divided into a control group, model group (10 μg/mL LPS intervention for 12 h, and 8 mM ATP intervention for 2 h), and KR group (after pretreatment of 25 μM KR for 12 h, 10 μg/mL LPS intervention for 12 h, and 8 mM ATP intervention for 2 h).

Molecular docking

The structure of KR was downloaded from PubChem (https://pubchem.ncbi.nlm.nih.gov/) which was processed by adding hydrogens and partial charges. TXNIP (PDB: 4GEI) was obtained from RCSB (https://www.rcsb.org/) (Polekhina *et al*., 2013). To obtain the sizes of the docking box, distances between the center and each atom along the three axes (x, y, and z) were calculated. CB-DOCK (http://clab.labshare.cn/cb-dock/) was used to predict the binding affinity of the chemical and target (Liu *et al.*, 2020).

Determination of enzymology parameters

The LDH activity in cell supernatants was measured according to the manufacturer's instructions. T-SOD (550 nm), MDA (532 nm), GSH (405 nm), and CAT (405 nm) activities were measured by colorimetric assay.

Detection of cellular ROS levels

H9c2 cells were inoculated into 6-well plates at 90% density, with a density of 3×10^5 cells/well. After treatment in groups, they were mixed with 10 μM DCFH-DA and incubated in a serum-free medium for 15 min. After washing with PBS, the fluorescence intensity was observed with a fluorescence microscope (Olympus IX81, Japan).

RT-qPCR for mRNA expression

H9c2 cells were inoculated at a density of 2×10^5 cells in 6-well plates and cultured for 24 h. The mRNA assay was conducted based on the methods described in a previous study (Yang *et al.*, 2024). The amplification procedure includes the following: pre-denaturing at 95°C for 5 min, then denaturing at 95°C for 15 s, annealing at 60°C for 60 s, and performing 40 cycles of PCR. The melting curve is from 60°C to 95°C. The mRNA expression levels of the genes were analyzed using the $2^{-\Delta\Delta Cq}$ method with β-actin as a reference control. The primer sequence for TXNIP (Forward: 5′-CCAGACCAAAGTGCTCACTCAGAAG-3′, Reverse: 5′-GAGACTCTTGCCACGCCATGATG-3′), TRX (Forward: 5′-AAGCCCTTCTTTCATTCCCTCTG TG-3′, Reverse: 5′-CAGCAACATCCTGGCAGTCA TCC-3′), NLRP3 (Forward: 5′-GAGCTGGACCTCAG TGACAATGC-3′, Reverse: 5′-AGAACCAATGCGAGA TCCTGACAAC-3′), Caspase-1 (Forward: 5′-GCACAA GACTTCTGACAGTACCTTCC-3′, Reverse: 5′-GCTTG GGCACTTCAATGTGTTCATC-3′), and β-actin (Forward: 5′-CCCATCTATGAGGGTTACGC-3′, Reverse: 5′-TTTAATGTCACGCACGATTTC-3′) were used in the study.

Western blot for protein expression

H9c2 cells were seeded in 6-well plates at a density of 2×10^5 cells per well and cultured for 24 h. Equal amounts of total protein were separated using 10%–12% SDS-PAGE and transferred to a PDVF membrane following protein quantification with a BCA kit. The membrane was blocked with 5% skim milk for 2 h. After blocking, the membrane was incubated with primary antibodies overnight at 4 °C following three washes with TBST solution. The protein assay was performed according to a previous study (Hua *et al.*, 2022). TXNIP (1:1000), TRX (1:500), NLRP3 (1:1000), Cleaved-caspase-1 (1:1000), and GAPDH (1:5000) were incubated at 4°C overnight. The protein bands were photographed using the Tanon5200 imaging system (Tanon, China), and the optical density values of the bands were analyzed using ImageJ software.

ELISA for the expression of IL-1β and IL-18

IL-1β and IL-18 levels in rat serum were detected by test kits. Fluorescence was measured on a SpectraMax i3x (Molecular Devices, USA) microplate reader at 450 nm.

Statistical analysis

The data were presented as mean ± standard deviation, and statistical analysis was conducted using SPSS 26.0. One-way ANOVA was performed, and the results indicated that a P-value of less than 0.05 was considered statistically significant.

Results

Molecule docking for KR

The lower the Vina score, the stronger the binding affinity between KR and TXNIP. Verapamil had a Vina score of 5.5, while KR had a score of -6.7, indicating that the binding affinity of KR to TXNIP was higher than that of the TXNIP inhibitor. KR had a good binding affinity to TXNIP, suggesting that KR may act on TXNIP (Table 1, Figure 1), as supported by cellular experiments.

Table 1. Docking scores of KR with TXNIP targets.

Chemicals	Vina score	Cavity score	Center (x, y, z)	Size (x, y, z)
Verapamil	–5.5	555	17, 39, –8	27, 27, 27
KR	–6.7	555	17, 39, –8	26, 26, 26

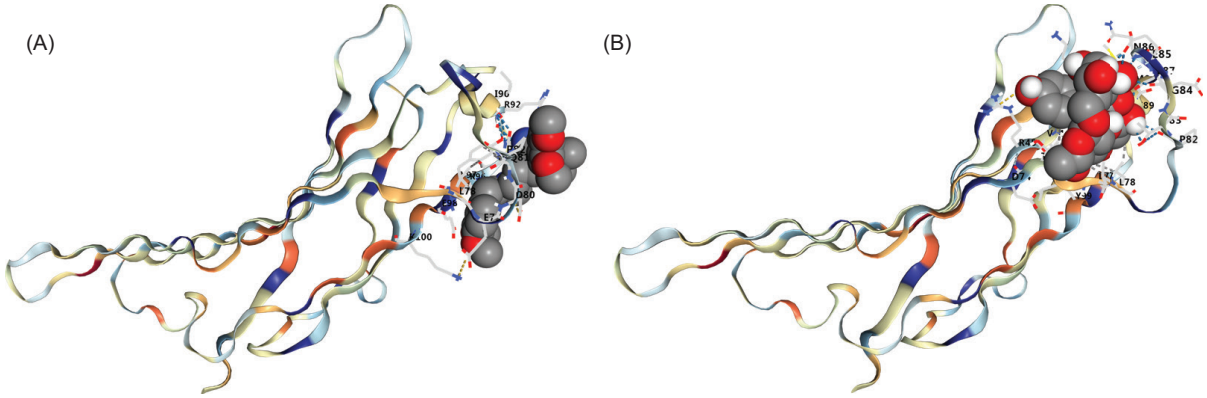

Figure 1. Docking of KR to TXNIP. (A) Verapamil (B) KR.

Effect of LGZGD on LDH activity

LDH activity was significantly higher in the model group (P<0.01), and KR could decrease the LDH activity (P<0.01) (Figure 2). The results indicated that KR intervention could effectively ameliorate the myocardial injury caused by LPS+ATP on H9c2 cells.

Effect of LGZGD on cellular oxidative stress

In the model group, CAT, GSH, and T-SOD activities were significantly lower, while MDA content was significantly higher (P<0.01). However, following KR intervention, these oxidative stress indicators were notably reversed (P<0.01) (Figure 3).

Effect of KR on the level of ROS

The effect of KR on ROS was assessed using a kit in H9c2 cells. Induction with LPS+ATP significantly increased ROS production in the model group (P<0.01). However, ROS production was significantly inhibited following KR intervention (P<0.01) (Figure 4).

KR inhibited the expression of key genes

In the model group, gene expression levels of TXNIP, Caspase-1, and NLRP3 were significantly increased, and TRX gene expression was significantly decreased (P<0.01). However, in the KR group, these gene expressions were significantly reduced, and TRX gene expression was significantly increased (P<0.01) (Figure 5).

KR inhibited the expression of key proteins

In the model group, protein expression levels of TXNIP, Cleaved-caspase-1, and NLRP3 were significantly

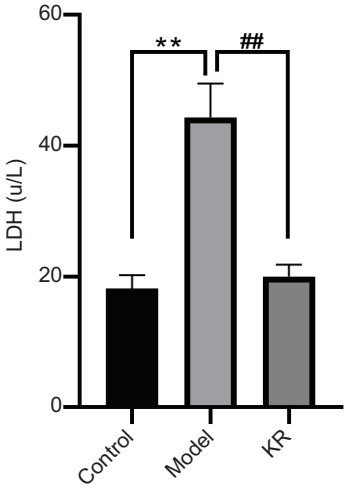

Figure 2. Effect of LGZGD on LDH activity. Compared with the control group, **$P < 0.01$; compared with the model group, ##$P < 0.01$.

elevated, while TRX protein expression was decreased (P<0.01). After KR treatment, these protein expression levels were significantly reversed (P<0.01) (Figure 6).

KR improved IL-1β and IL-18 in myocardial injury

In the model group, the levels of IL-1β and IL-18 were significantly increased (P<0.01). In contrast, KR treatment significantly suppressed these inflammation levels (P<0.01) (Figure 7).

Discussion

TXNIP is a marker associated with metabolism, oxidation, and inflammation in cardiovascular diseases (CVDs). Its overexpression is closely linked to the onset and progression of CVDs (Zhou *et al.*, 2023). Inhibiting TXNIP is crucial for mitigating the excessive activation of

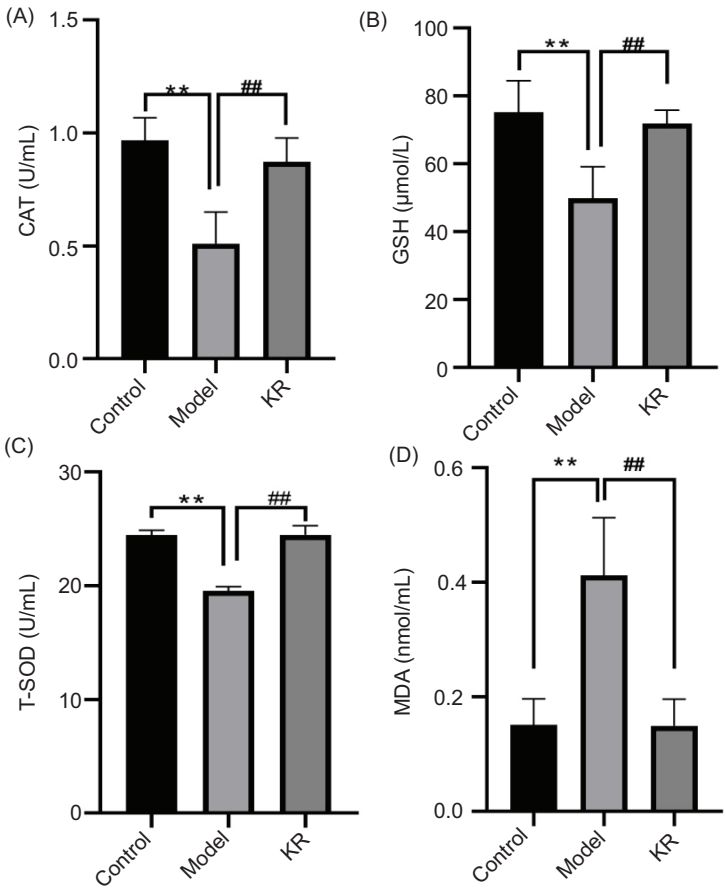

Figure 3. Effect of LGZGD on cellular oxidative stress. (A) CAT; (B) GSH; (C) T-SOD; (D) MDA. Compared with the control group, **$P < 0.01$; compared with the model group, $^{\#\#}P < 0.01$.

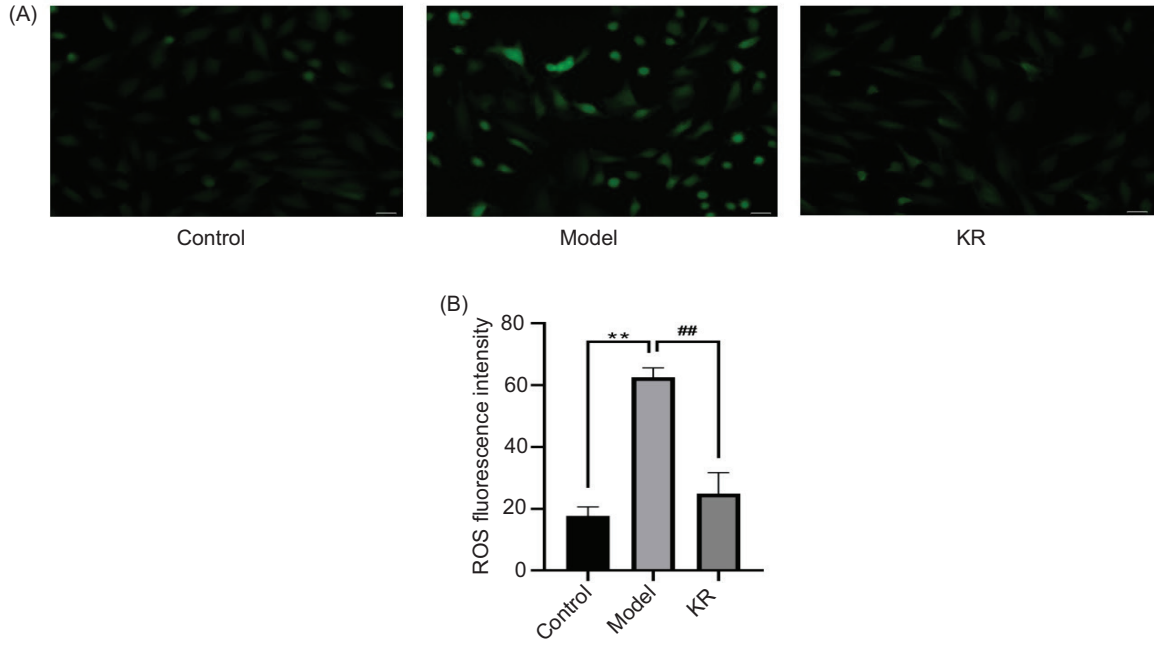

Figure 4. Effect of KR on the level of ROS. (A) Representative image (B) Quantitative analysis. Compared with the control group, **$P < 0.01$; compared with the model group, $^{\#\#}P < 0.01$.

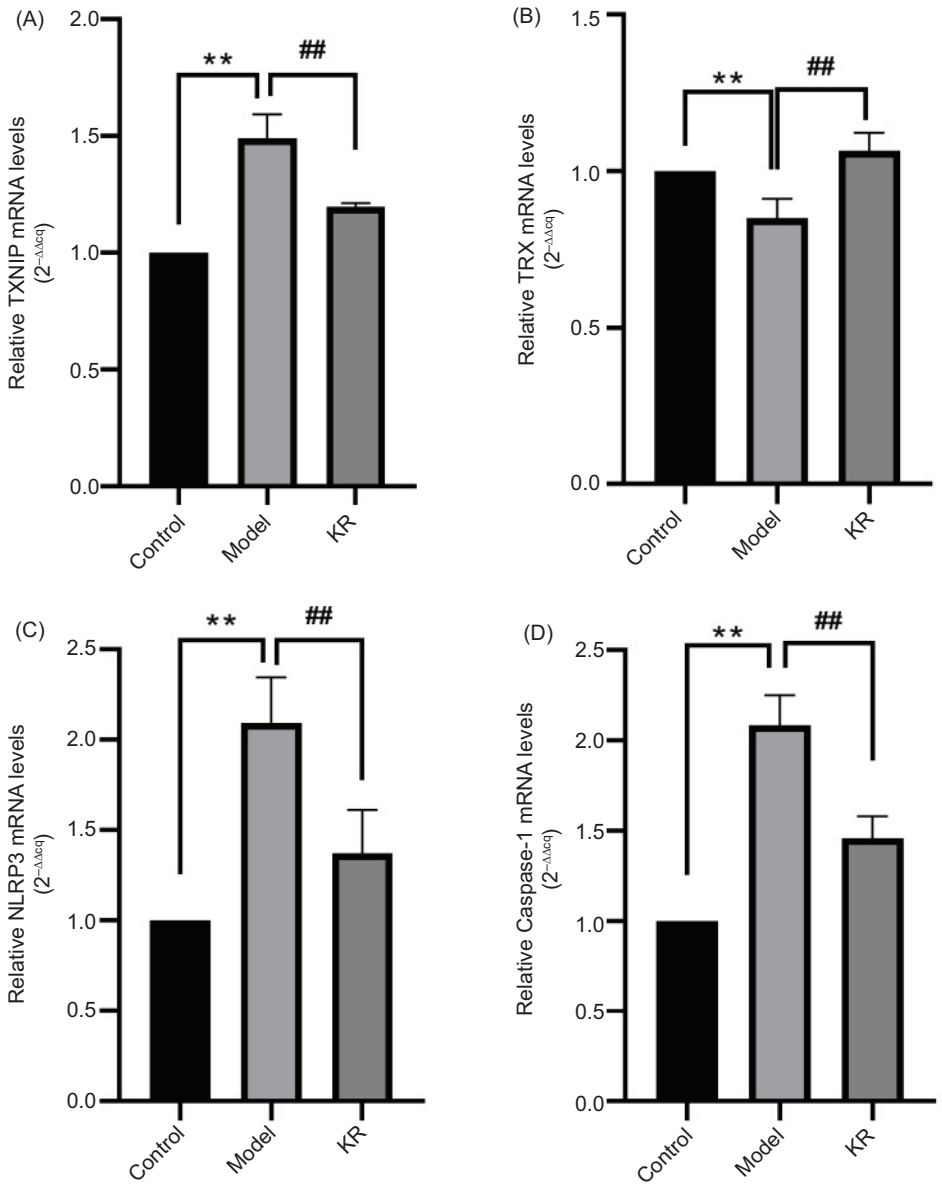

Figure 5. KR inhibited the expression of key genes. (A) TXNIP; (B) TRX; (C) NLRP3; (D) Caspase-1. Compared with the control group, **$P < 0.01$; compared with the model group, ##$P < 0.01$.

downstream signaling pathways, thereby reducing myocardial cell damage (Xi *et al.*, 2024). TXNIP also interacts with NLRP3, which activates NLRP3 inflammasome and promotes inflammatory processes, including pyroptosis (Bharti *et al.*, 2019; Luo *et al.*, 2022).

Pyroptosis is a form of programmed cell death characterized by the continuous swelling of cells until their membranes rupture. This process leads to the release of cellular contents and activation of a potent inflammatory cascade (de Torre-Minguela *et al.,* 2021; Zhang *et al*., 2024). It is an important natural immune response, dependent on Caspase-1, and involves the release of pro-inflammatory factors. Pyroptosis can be detected by measuring the levels of intracellular expression of inflammatory factors and Caspase-1 proteins (Toldo and Abbate, 2024). The NLRP3/Caspase-1 pathway is one of the classical pathways of cellular pyroptosis, involving several key components: NLRP3, Caspase-1, ASC, GSDMD, and GSDMD-N (Imre, 2024).

Upon stimulation by pyroptosis signals, intracellular pattern recognition receptors bind to pattern recognition molecules. NLRP3, initially inactivate in the cytoplasm, undergoes oligomerization upon relevant stimulation, which is a crucial step for its activation. The PYD structural domain of NLRP3 binds to the PYD structural domain of ASC, while the CARD structural domain

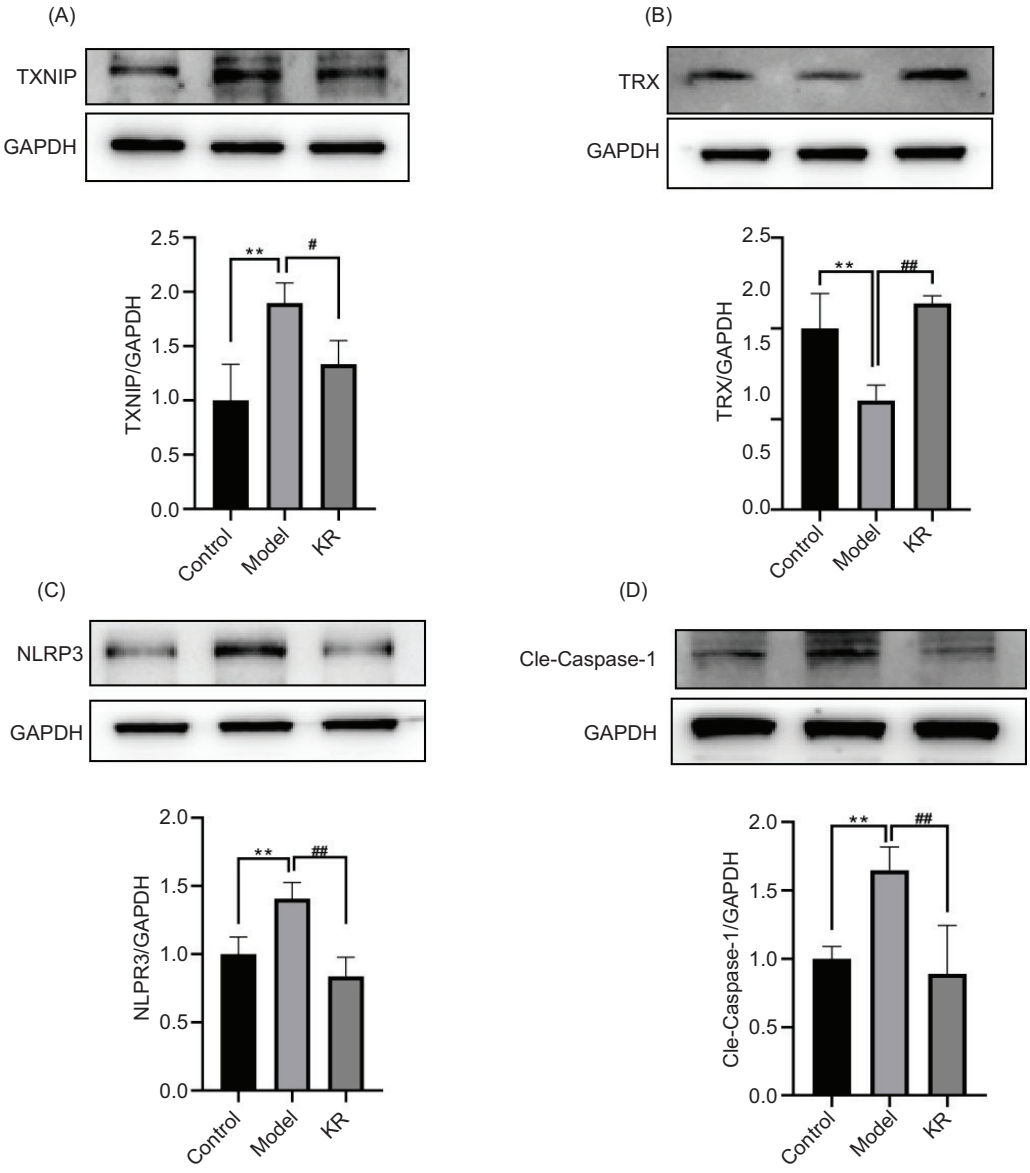

Figure 6. KR inhibited the expression of key proteins. (A) TXNIP; (B) TRX; (C) NLRP3; (D) Cleaved-caspase-1. Compared with the control group, $^{**}P < 0.01$; compared with the model group, $^{\#\#}P < 0.01$.

of ASC binds to the CARD structural domain of pro-Caspase-1, leading to the formation of the NLRP3 inflammasome (NLRP3-ACS-proCaspase-1). Upon activation of the NLRP3 inflammasome, caspase-1 is activated and specifically cleaves the precursors of IL-1β and IL-18, conveting them into their active forms. This process triggers an inflammatory cascade and induces cellular pyroptosis (Abbate and Booz, 2019; Li *et al*., 2022; Liang *et al*., 2020). During myocardial ischemia, large amounts of ROS are generated, playing a crucial role in oxidative stress and acting as key regulators of the NLRP3 inflammasome. At the onset of AMI, damage-associated molecular patterns (DAMPs)-induced ROS stimulate the detachment of TXNIP from its binding partner, TRX. TXNIP then translocates from the nucleus to the cytoplasm, where it binds to NLRP3, leading to the activation of the NLRP3 inflammasome. This activation results in the activation of Caspase-1, which cleaves the precursors of IL-1β and IL-18 into their active forms. These active cytokines then trigger cellular pyroptosis (Qiu *et al.*, 2019; Sukhanov *et al*., 2021). Inhibition of NLRP3 using small interfering RNA (siRNA) in animal models of permanent myocardial infarction has been shown to suppress inflammasome activation, reduce cardiomyocyte death, and attenuate VR after AMI (Mezzaroma *et al*., 2011). After the establishment of myocardial ischemia/reperfusion model using ASC knockout mice (ASC-/-mice) and Caspase-1 knockout mice (Caspase-1-/-mice), it was found that the inflammatory response was significantly reduced compared to wild-type mice. This reduction was evidenced

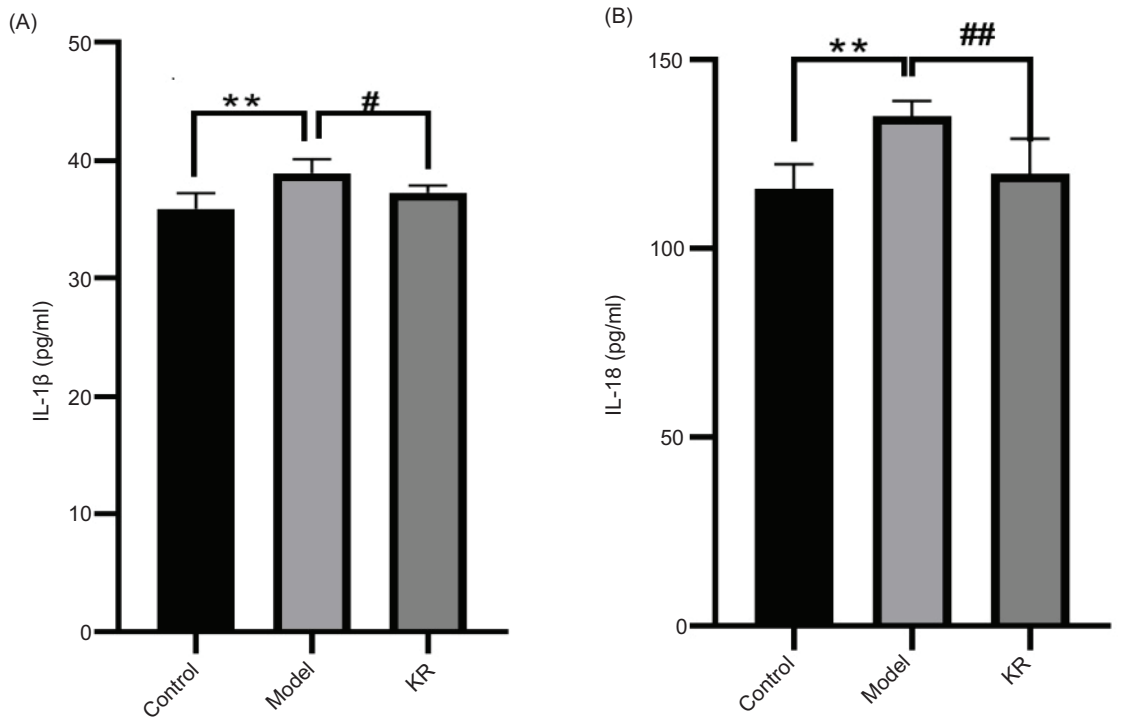

Figure 7. KR improved IL-1β and IL-18 in myocardial injury. (A) IL-1β; (B) IL-18. Compared with the control group, $^{**}P < 0.01$, Compared with the model group, $^{\#\#}P < 0.01$.

by decreased inflammatory cell infiltration, lower expression of cytokines and chemokines, and a smaller myocardial infarction area in the knockout mice (Kawaguchi *et al.*, 2011).

In this study, CB-dock was used to predict the binding affinity of KR to TXNIP. CB-dock can automatically predict binding modes without prior binding site information by using a novel curvature-based cavity detection approach to identify potential binding sites and calculate the center and size of the binding site (Liu *et al.*, 2020). The molecular docking results showed that KR had a better binding affinity with TXNIP. The experimental results of this study demonstrated that NLRP3 expression significantly increased after combined LPS+ATP modeling, indicating successful model establishment. KR significantly reduced oxidative stress injury and decreased the expression of cellular pyroptosis-related proteins and genes in H9c2 cells, suggesting that the cardioprotective effect of KR is associated with the inhibition of the ROS/NLRP3 signaling pathway. Although this study provides insights into the cardioprotective mechanism of KR, it only established a correlation between KR and myocardial protection. The detailed mechanisms were not clarified using specific agonists or gene overexpression techniques.

In conclusion, the mechanism by which KR protects cardiomyocytes from injury is related to the inhibition of the TXNIP/NLRP3 pathway. This provides a theoretical and experimental basis for its possible clinical application.

Conflicts of Interest

The authors declare that they have no conflicts of interest.

Acknowledgments

This study was supported by the Outstanding Youth Scientific Research Project of Anhui Universities (2022AH030158), the Teaching Team Project of Anhui Xinhua University (2022jxtdx03), and the Pharmaceutical Institute of Anhui Xinhua University (yjs202107).

References

Abbate, A., & Booz, G. W. (2019). Cardiovascular pharmacology of the NLRP3 inflammasome. Journal of Cardiovascular Pharmacology, 74, 173–174. https://doi.org/10.1097/FJC.0000000000000725c

Bai, W. X., Wang, C., Wang, Y. J., Zheng, W. J., Wang, W., Wan, X. C., et al. (2017). Novel acylated flavonol tetraglycoside with inhibitory effect on lipid accumulation in 3T3-L1 cells from Lu'an GuaPian tea and quantification of flavonoid glycosides in six major processing types of tea. Journal of Agricultural and

Food Chemistry, 65, 2999–3005. https://doi.org/10.1021/acs.jafc.7b00239

Bharti, V., Tan, H., Zhou, H., & Wang, J. F. (2019). TXNIP mediates glucocorticoid-activated NLRP3 inflammatory signaling in mouse microglia. Neurochemistry International, 131, 104564. https://doi.org/10.1016/j.neuint.2019.104564

Cheng, Y. C., Chu, L.W., Chen, J. Y., Hsieh, S. L., Chang, Y. C., Dai, Z. K., et al. (2020). Loganin attenuates high glucose-induced Schwann cells pyroptosis by inhibiting ROS generation and NLRP3 inflammasome activation. Cells, 9, 1948. https://doi.org/10.3390/cells9091948

de Torre-Minguela, C., Gómez, A. I., Couillin, I., & Pelegrín, P. (2021). Gasdermins mediate cellular release of mitochondrial DNA during pyroptosis and apoptosis. FASEB Journal, 35, e21757. https://doi.org/10.1096/fj.202100085R

Dubey, R., & Dubey, K. (2021). Molecular docking studies of bioactive nicotiflorin against 6W63 novel coronavirus 2019 (COVID-19). Combinatorial Chemistry & High Throughput Screening, 24, 874–878. https://doi.org/10.2174/1386207323999200820162551

Frangogiannis, N. G. (2014). The inflammatory response in myocardial injury, repair, and remodelling. Nature Reviews Cardiology, 11, 255–265. https://doi.org/10.1038/nrcardio.2014.28

Guedes, I. A., de Magalhães, C. S., & Dardenne L. E. (2014). Receptor-ligand molecular docking. Biophysical Reviews, 6, 75–87. https://doi.org/10.1007/s12551-013-0130-2

Hua, F., Zhou, P., Liu, P. P., & Bao, G. H. (2021). Rat plasma protein binding of kaempferol-3-O-rutinoside from Lu'an GuaPian tea and its anti-inflammatory mechanism for cardiovascular protection. Journal of Food Biochemistry, 45, e13749. https://doi.org/10.1111/jfbc.13749

Hua, F., Zhou, P., Wu, H. Y., Chu, G. X., Xie, Z. W., & Bao, G. H. (2018). Inhibition of α-glucosidase and α-amylase by flavonoid glycosides from Lu'an GuaPian tea: Molecular docking and interaction mechanism. Food & Function, 9, 4173–4183. https://doi.org/10.1039/C8FO00562A

Hua, F., Li, J. Y., Zhang, M., Zhou, P., Wang, L., Ling, T. J., et al. (2022). Kaempferol-3-O-rutinoside exerts cardioprotective effects through NF-κB/NLRP3/Caspase-1 pathway in ventricular remodeling after acute myocardial infarction.Journal of Food Biochemistry, 46, e14305. https://doi.org/10.1111/jfbc.14305

Imre, G. (2024). Pyroptosis in health and disease. American Journal of Physiology-Cell Physiology, 326, C784–C794. https://doi.org/10.1152/ajpcell.00503.2023

Kawaguchi, M., Takahashi, M., Hata, T., Kashima, Y., Usui, F., Morimoto, H., et al. (2011). Inflammasome activation of cardiac fibroblasts is essential for myocardial ischemia/reperfusion injury. Circulation, 123, 594–604. https://doi.org/10.1161/CIRCULATIONAHA.110.982777

Li, H., Guan, Y., Liang, B., Ding, P., Hou, X., & Wei, W. (2022). Therapeutic potential of MCC950, a specific inhibitor of NLRP3 inflammasome. European Journal of Pharmacology, 928, 175091. https://doi.org/10.1016/j.ejphar.2022.175091

Liang, F., Zhang, F., Zhang, L., & Wei, W. (2020). The advances in pyroptosis initiated by inflammasome in inflammatory and immune diseases. Inflammation Research, 69, 159–166. https://doi.org/10.1007/s00011-020-01315-3

Liu, Y., Grimm, M., Dai, W. T., Hou, M. C., Xiao, Z. X., & Cao, Y. (2020). CB-Dock: A web server for cavity detection-guided protein-ligand blind docking. Acta Pharmacologica Sinica, 41, 138–144. https://doi.org/10.11648/j.cb.20200802.13

Luo, T., Zhou, X., Qin, M., Lin, Y., Lin, J., Chen G., et al. (2022). Corilagin restrains NLRP3 inflammasome activation and pyroptosis through the ROS/TXNIP/NLRP3 pathway to prevent inflammation. Oxidative Medicine and Cellular Longevity, 2022, 1652244. https://doi.org/10.1155/2022/1652244

Mezzaroma, E., Told,o S., Farkas, D., Seropian, I. M., Van Tassell, B. W., Salloum, F. N., et al. (2011). The inflammasome promotes adverse cardiac remodeling following acute myocardial infarction in the mouse. Proceedings of the National Academy of Sciences USA, 108, 1972–-19730. https://doi.org/10.1073/pnas.1108586108

Palasubramaniam, J., Wang, X., & Peter, K. (2019). Myocardial infarction – From atherosclerosis to thrombosis. Arteriosclerosis, Thrombosis, and Vascular Biology, 39, e176–e185. https://doi.org/10.1161/ATVBAHA.119.312578

Petpiroon, N., Suktap, C., Pongsamart, S., Chanvorachote, P., & Sukrong, S. (2015). Kaempferol-3-O-rutinoside from Afgekia mahidoliae promotes keratinocyte migration through FAK and Rac1 activation. Journal of Natural Medicines, 69, 340–348. https://doi.org/10.1007/s11418-015-0899-3

Polekhina, G., Ascher, D. B., Kok, S. F., Beckham, S., Wilce, M., & Waltham, M. (2013). Structure of the N-terminal domain of human thioredoxin-interacting protein. Acta Crystallographica. Section D, Biological Crystallography, 69, 333–344. https://doi.org/10.1107/S0907444912047099

Qiu, Z., He, Y., Ming, H., Lei, S., Leng, Y., & Xia, Z. Y. (2019). Lipopolysaccharide (LPS) aggravates high glucose- and hypoxia/reoxygenation-induced injury through activating ROS-dependent NLRP3 inflammasome-mediated pyroptosis in H9C2 cardiomyocytes. Journal of Diabetes Research, 2019, 8151836. https://doi.org/10.1155/2019/8151836

Sukhanov, S., Higashi, Y., Yoshida, T., Mummidi, S., Aroor, A. R., Jeffrey Russell, J., et al. (2021). The SGLT2 inhibitor empagliflozin attenuates interleukin-17A-induced human aortic smooth muscle cell proliferation and migration by targeting TRAF3IP2/ROS/NLRP3/Caspase-1-dependent IL-1β and IL-18 secretion. Cell Signalling, 77, 109825. https://doi.org/10.1016/j.cellsig.2020.109825

Toldo, S., & Abbate, A. (2024). The role of the NLRP3 inflammasome and pyroptosis in cardiovascular diseases. Nature Reviews Cardiology, 21, 219–237. https://doi.org/10.1038/s41569-023-00946-3

Wang, D. S., Yan, L. Y., Yang, D. Z., Lyu, Y., Fang, L. H., Wang, S. B., et al. (2020). Formononetin ameliorates myocardial ischemia/reperfusion injury in rats by suppressing the ROS-TXNIP-NLRP3 pathway. Biochemical and Biophysical Research Communications, 525, 759–766. https://doi.org/10.1016/j.bbrc.2020.02.147

Wang, Y., Tang, C., & Zhang, H. (2015). Hepatoprotective effects of kaempferol 3-O-rutinoside and kaempferol 3-O-glucoside from Carthamus tinctorius L. on CCl_4-induced oxidative liver injury in mice. Journal of Food and Drug Analysis, 23, 310–317. https://doi.org/10.1016/j.jfda.2014.10.002

Xi, X., Zhang, R., Chi, Y., Zhu, Z., Sun, R., & Gong, W. (2024). TXNIP regulates NLRP3 inflammasome-induced pyroptosis related to aging via cAMP/PKA and PI3K/Akt signaling pathways. Molecular Neurobiology, doi: 10.1007/s12035-024-04089-5 [Online ahead of print]. https://doi.org/10.1007/s12035-024-04089-5

Yang, Y. L., Zhao, C. Z., Zhao, C. C., Wen, Z. Y., Ma, Y. Y., & Zhao, X. N. (2024). Ling-Gui-Zhu-Gan decoction protects against doxorubicin-induced myocardial injury by downregulating ferroptosis. Journal of Pharmacy and Pharmacology, 76, 405–415. https://doi.org/10.1093/jpp/rgae005

Yoshihara, E., Matsuo, Y., Masaki, S., Chen, Z., Tian, H., Masutani, H., et al. (2024). Redoxisome update: TRX and TXNIP/TBP2-dependent regulation of NLRP-1/NLRP-3 inflammasome. Antioxidants & Redox Signaling, 40, 595–597. https://doi.org/10.1089/ars.2024.0549

Zhang, Y., Zhao, H., Fu, X., Wang, K., Yang, J., Zhang, X., et al. (2024). The role of hydrogen sulfide regulation of pyroptosis in different pathological processes. European Journal of Medicinal Chemistry, 268, 116254. https://doi.org/10.1016/j.ejmech.2024.116254

Zhao, H., Lin, X., Chen, Q., Wang, X., Wu, Y., & Zhao, X. (2023). Quercetin inhibits the NOX2/ROS-mediated NF-κB/TXNIP signaling pathway to ameliorate pyroptosis of cardiomyocytes to relieve sepsis-induced cardiomyopathy. Toxicology and Applied Pharmacology, 477, 116672. https://doi.org/10.1016/j.taap.2023.116672

Zheng, Z., Lei, C., Liu, H., Jiang, M., Zhou, Z., Zhao, Y., et al. (2022). A ROS-responsive liposomal composite hydrogel integrating improved mitochondrial function and pro-angiogenesis for efficient treatment of myocardial infarction. Advanced Healthcare Materials, 11, e2200990. https://doi.org/10.1002/adhm.202200990

Zhou, P., Ma, Y. Y., Zhao, X. N., & Hua F. (2023). Phytochemicals as potential target on thioredoxin-interacting protein (TXNIP) for the treatment of cardiovascular diseases. Inflammopharmacology, 31, 207–220. https://doi.org/10.1007/s10787-022-01130-8

Zhu, L., Yang, Y. M., Huang, Y., Xie, H. K., Luo, Y., Li, C., et al. (2024). Shexiang Tongxin dropping pills protect against ischemic stroke-induced cerebral microvascular dysfunction via suppressing TXNIP/NLRP3 signaling pathway. Journal of Ethnopharmacology, 322, 117567. https://doi.org/10.1016/j.jep.2023.117567